DOI: http://dx.doi.org/10.12989/sem.2007.26.6.709

New method for generation of artificial ground motion by a nonstationary Kanai-Tajimi model and wavelet transform

G. Ghodrati Amiri†, A. Bagheri‡ and M. Fadavi‡†

Center of Excellence for Fundamental Studies in Structural Engineering, College of Civil Engineering, Iran University of Science & Technology, PO Box 16765-163, Narmak, Tehran 16846, Iran

(Received July 21, 2006, Accepted March 22, 2007)

Abstract. Considering the vast usage of time-history dynamic analyses to calculate structural responses and lack of sufficient and suitable earthquake records, generation of artificial accelerograms is very necessary. The main target of this paper is to present a novel method based on nonstationary Kanai-Tajimi model and wavelet transform to generate more artificial earthquake records, which are compatible with target spectrum. In this regard, the generalized nonstationary Kanai-Tajimi model to include the nonstationary evaluation of amplitude and dominant frequency of ground motion and properties of wavelet transform is used to generate ground acceleration time history. Application of the method for El Centro 1940 earthquake and two Iranian earthquakes (Tabas 1978 and Manjil 1990) is presented. It is shown that the model and identification algorithms are able to accurately capture the nonstationary features of these earthquake accelerograms. The statistical characteristics of the spectral response of the generated accelerograms are compared with those for the actual records to demonstrate the effectiveness of the method. Also, for comparison of the presented method with other methods, the response spectra of the synthetic accelerograms compared with the models of Fan and Ahmadi (1990) and Rofooei *et al.* (2001) and it is shown that the response spectra of the synthetic accelerograms with the method of this paper are close to those of actual earthquakes.

Keywords: artificial accelerogram; wavelet transform; target spectrum; nonstationary model; Kanai-Tajimi model.

1. Introduction

Dynamic response analysis of structures to earthquake ground motion is one of the basic requirements for their seismic design. While response spectra method is the currently favored approach, there are situations for which a time history analysis is necessary. Typical examples are qualification of sensitive equipment, evaluation of floor response, and response analysis of nonlinear structures and structural components. The number of recorded accelerograms, however, is too limited to allow the selection of a standard typical record for a given site. Furthermore, under

† Associate Professor, Corresponding author, E-mail: ghodrati@iust.ac.ir
‡ M.Sc. Student, E-mail: abaghery@civileng.iust.ac.ir
‡† M.Sc. Student, E-mail: fadavi@comp.iust.ac.ir

seemingly similar conditions, considerable variations in the features of ground shaking are observed. Thus, there is need for generating ensembles of realistic artificial earthquake ground motion records to cover a variety of uncertainties in seismic design of structures (Fan and Ahmadi 1990). A review of early works for generation of artificial time-histories compatible with given response spectra can be found in Ahmadi (1979).

Because of the complex nature of the formation of seismic waves and their travel path before reaching recording station, a stochastic approach may be most suitable for generation artificial accelerograms. In this concern, different stochastic models, both stationary and nonstationary have broadly been widely used in literature to simulate earthquake ground motions. The stationary filtered white noise model of earthquake ground motion of Kanai and Tajimi has attracted considerable attention, and was extensively used in random vibration analysis of structures (Kanai 1957, Tajimi 1960). More recent models to include the nonstationary variations in amplitude and frequency content were suggested (Fan and Ahmadi 1990, Refooei *et al.* 2001).

The newly developed wavelet analysis has emerged as a powerful tool to analyze temporal variations in frequency content. Recent applications of the wavelet transform to engineering problems can be found in several studies that refer to dynamic analysis of structures, damage detection, system identification, etc. Newland (1994) applied wavelets for analyzing vibration signals, and developed special wavelets and techniques for engineering purpose. Ghodrati Amiri *et al.* (2006), Suarez and Montejo (2005), Mukherjee and Gapta (2002), Iyama and Kuwamura (1999) developed the wavelet analysis for generating earthquake accelerograms.

In this study, an effective method for generation of artificial accelerograms for any site with at least one existing earthquake record is presented. Specific examples of El Centro 1940, Tabas 1978 and the Manjile 1990 earthquakes are demonstrated in detail. It is shown that the generate accelerograms preserve the time dependent frequency content of the original records. The response spectra curves for the generated earthquakes are also compared with those of the original records and discussed.

2. Generalized Kanai-Tajimi model

Based on Kanai's investigation regarding the frequency content of different earthquake records, Tajimi proposed Relation (1) for the spectral density function of the strong motion with a distinct dominant frequency

$$S(\omega) = \frac{1 + 4\xi_g^2(\omega/\omega_g)^2}{[1-(\omega/\omega_g)^2] + 4\xi_g^2(\omega/\omega_g)^2} S_0 \tag{1}$$

In which ξ_g and ω_g are site dominant damping coefficient and frequency, and S_0 is the constant power spectral intensity of bedrock excitation. In practice these parameters need to be estimated from the local earthquake recodes and geological features. Kanai-Tajimi power spectral density function may be commented as corresponding to an 'ideal white noise' excitation at bedrock level filtered through the overlaying soil deposits at a site. The most serious shortcoming of the original Kanai-Tajimi model is its behavior of earthquake as stationary random processes. An improved version of the model was introduced by Fan and Ahmadi (1990) to capture the nonstationary feature of real earthquake records. This generalized nonstationary Kanai-Tajimi model is represented Eqs. (2) and (3)

$$\ddot{X}_f + 2\xi_g(t)\omega_g(t)\dot{X}_f + \omega_g^2(t)X_f = n(t) \tag{2}$$

$$\ddot{X}_g = -(2\xi_g(t)\omega_g(t)\dot{X}_f + \omega_g^2(t)X_f)e(t) \tag{3}$$

Where X_f is filtered response, $\omega_g(t)$ is time dependent ground frequency, $\xi_g(t)$ is effective ground damping coefficient, $\ddot{X}_g$ is output ground acceleration, and $e(t)$ is amplitude envelope function. In Eq. (3), $n(t)$ is a stationary Gaussian white noise process with the parameters in Eq. (4).

$$E[n(t)] = 0, \qquad E[n(t_1)n(t_2)] = 2\pi S_0\delta(t_1 - t_2) \tag{4}$$

Where $E[]$ stands for expected value, and $\delta()$ is Dirac delta function. For $e(t) = 1$, and $\omega_g(t)$ and $\xi_g(t)$ being constants, Eqs. (2)-(4) reduce to the original Kanai-Tajimi model. In this case the power spectral density of ground acceleration is given by Eq. (1).

Eqs. (2)-(4) provide filtered white noise stochastic time series with appropriate frequency content and amplitude modulation for ground acceleration during earthquake.

3. Wavelet theory

3.1 Basis function

Fast Fourier transform (FFT) is a perfect tool for finding the frequency components in a signal. A disadvantage of the FFT is that frequency components can only be extracted from the complete duration of a signal. The frequency components are obtained from an average over the whole length of the signal. Therefore it is not a suitable tool for a non-stationary signal such as the impulse response of cracked beams, vibration generated by faults in a gearbox, and structural response to wind storms, just to name a few. These types of problems associated with FFT can be resolved by using wavelet analysis. It provides a powerful tool to characterize local features of a signal. Unlike Fourier transform, where the function used as the basis of decomposition is always a sinusoidal wave, other basis functions can be selected for wavelet shape according to the features of the signal. The basis function in wavelet analysis is defined by two parameters named scale and translation. This property leads to a multi-resolution representation for non-stationary signals. As mentioned before, a basis function (or mother wavelet) is used in wavelet analysis. For a wavelet of order N, the basis function can be represented as

$$\psi(n) = \sum_{j=0}^{N-1}(-1)^j c_j(2n + j - N + 1) \tag{5}$$

where c_j is jth coefficient. The basis function should satisfy the following two conditions (Relations (6) and (7)):

The basis function integrates to zero, i.e.

$$\int_{-\infty}^{+\infty}\psi(t)dt = 0 \tag{6}$$

It is square integrable or, equivalently, has finite energy, i.e.

$$\int_{-\infty}^{+\infty} |\psi(t)|^2 dt < \infty \tag{7}$$

Eq. (6) suggests that the basis function be oscillatory or have a wavy shape. Eq. (7) implies that most of the energy in the basis function is confined to a finite duration. The important properties of basis functions are 'orthogonality' and 'biorthogonality'. These properties make it possible to calculate the coefficients very efficiently. There is no redundancy in the sense that there is only one possible wavelet decomposition for the signal being analyzed. However, not all basis functions have these properties. A frequently mentioned term in the definition of a basis function is 'compact support', which means that the values of the basis function are non-zero for finite intervals. This property enables one to efficiently represent signals that have localized features.

3.2 Continuous wavelet transform (CWT)

The CWT is defined as

$$W_{a,b} = \frac{1}{\sqrt{a}} \int_{-\infty}^{+\infty} f(t)\, \psi^*\left(\frac{t-b}{a}\right) dt \tag{8}$$

Where a and b are scale and translation parameters, respectively and ψ^* is the complex conjugate of ψ. The basis function ψ is represented as

$$\psi_{j,k}(t) = 2^{j/2}\psi(2^j t - k) \tag{9}$$

If the scaling parameter a is $0 < a << 1$, it results in very narrow windows and is appropriate for high frequency components in the signal $f(t)$. If the value of a is $a >> 1$, it results in very wide windows and is suitable for the low frequency components in the signal. According to the uncertainty principle (also known as Heisenberg inequality), the resolution in time and frequency has (Relation (10))

$$\Delta t \Delta f \geq \frac{1}{4\pi} \tag{10}$$

Δf is proportional to the center frequency f, which leads to Relation (11)

$$\frac{\Delta f}{f} = C \tag{11}$$

where C is a constant. Therefore, the time resolution becomes arbitrarily good at high frequencies, while the frequency resolution becomes arbitrarily good at low frequencies. This property helps to overcome the limitation of *Short Time Fourier Transforms* (STFT) in which the time-frequency resolution is fixed. In order for an inverse wavelet transform to exist, the mother wavelet should satisfy the admissibility condition defined as

$$\int_{-\infty}^{+\infty} \frac{|\Psi(\omega)|^2}{|\omega|} d\omega < \infty \tag{12}$$

where Ψ is the Fourier transform of ψ (Daubechies 1992). Eq. (8) can be represented as

$$W_{a,b} = \langle f(t), \psi^*_{a,b}(t) \rangle \tag{13}$$

Therefore, CWT is a collection of inner products of a signal $f(t)$ and the translated and dilated wavelets $\psi_{a,b}(t)$.

3.3 Discrete wavelet transform (DWT)

The main idea of DWT is the same as that of CWT. While CWT requires much calculation effort to find the coefficients at every single value of the scale parameter, DWT adopts dyadic scales and translations (i.e., scales and translations based on powers of two) in order to reduce the amount of computation, which results in better efficiency of calculation. Filters of different cutoff frequencies are used for the analysis of the signal at different scales. The signal is passed through a series of high-pass filters to analyze high frequencies, and through a series of low-pass filters to analyze low frequencies. In DWT the signals can be represented by approximations and details. The detail at level j is defined as

$$D_j(t) = \sum_{k \in Z} cD_{j,k}\psi_{j,k}(t) \tag{14}$$

where Z is the set of positive integers and $cD_{j,k}$ is *wavelet Coefficients* at level j which is defined as

$$cD_j(k) = \int_{-\infty}^{\infty} f(t)\,\psi_{j,k}(t)dt \tag{15}$$

The approximation at level j is defined as

$$A_j(t) = \sum_{k=-\infty}^{\infty} cA_j(k)\phi_{j,k}(t) \tag{16}$$

where $cA_{j,k}$ is *scaling Coefficients* at level j which is defined as

$$cA_j(k) = \int_{-\infty}^{\infty} f(t)\phi_{j,k}(t)dt \tag{17}$$

Finally, the signal $f(t)$ can be represented by

$$f(t) = A_J + \sum_{j \le J} D_j \tag{18}$$

As opposed to CWT where only a wavelet function is used, in DWT a scaling function is used, in addition to the wavelet function. These are related to low-pass and high-pass filters, respectively. The scaling function $\phi(t)$ must satisfy the following three conditions

1. It integrates to one

$$\int_{-\infty}^{+\infty} \phi(t)dt = 1 \tag{19}$$

2. It has unit energy

$$\int_{-\infty}^{+\infty} |\phi(t)|^2 dt = 1 \tag{20}$$

3. The set consisting of $\phi(t)$ and its integer translates are orthogonal

$$\langle \phi(t), \phi(t-n) \rangle = \delta(n) \tag{21}$$

The scaling function can also be represented as

$$\phi(n) = \sum_{j=0}^{N-1} c_j \phi(2n-j) \tag{22}$$

$$\phi_{j,k}(n) = 2^{j/2}\phi(2^j t - k) \tag{23}$$

Which are similar to Eqs. (5) and (9), respectively. Not all wavelet functions have scaling functions. Only orthogonal wavelets have their scaling functions. This DWT can be very useful for on-line health monitoring of structures, since it can efficiently detect the time of a frequency change caused by stiffness degradation. Further details about wavelet theory can be found in Daubechies (1992).

3.4 Wavelet energy spectrum (WES)

Traditional measures of earthquake energy input include the followings:

- The root mean square (RMS) of the strong phase of the ground acceleration
- The maximum energy response of a single degree-of-freedom (SDOF) system subjected to ground motions with no damping
- Fourier amplitude spectrum

Zhou and Adeli (2003) proposed Relation (24) for wavelet energy spectrum to represent the time-frequency evolution of earthquake energy input

$$E_{a,b} = \frac{|W_{a,b}|^2}{\pi} \tag{24}$$

where the coefficients $W_{a,b}$ are obtained by applying the continuous Mexican hat wavelet transform to the ground acceleration $a_g(t)$ as follows

$$W_{a,b} = \frac{1}{\sqrt{a}}\int_{-\infty}^{+\infty} a_g(t)\,\psi\left(\frac{t-b}{a}\right)dt \tag{25}$$

In Eq. (25), a is used for the scaling parameters to distinguish it from the ground acceleration a_g. The Mexican hat wavelet is used as the basis wavelet function ψ in Eq. (25). The constant π is included in Eq. (24) for the Mexican hat wavelet so that the Parseval's theorem can be extended to include the wavelet transform.

4. Proposed method

In this approach, time-varying parameters for dynamic version of the Kanai-Tajimi model are considered. In order to estimate the time-dependency of the filter parameters, at least one recorded accelerogram is needed. For this purpose the 'Moving-Time-Window' technique is used (Fan and

Ahmadi 1990). This method is based on the assumption that a nonstationary process can approximately be assumed to be stationary within a time-window with appropriate size. The time-window should be sufficiently short to capture the rapid changes in frequency content, but long enough to provide for stable estimation of parameters and the ability to capture significant low frequency components. In this study, the optimal window size is selected based on the frequency content of earthquake using a trial and error method. In the present study, $\xi_g(t)$ is assumed to be a constant, and the time-evolution of $\omega_g(t)$ and $e(t)$ are determined using the following steps:

Using a time-window that moves from the beginning to the end of accelerograms, the standard deviation of the envelope function within each time window is calculated as follows

$$\sigma = (E[X^2] - E[X]^2)^{1/2} \tag{26}$$

This value is assigned to the center point of each time window. Then, a smooth algebraic time function $\sigma_a(t)$ is fitted to the time variation of the standard deviation. Finally, the amplitude envelope function is defined as

$$e(t) = C_0 \sigma_a(t) \tag{27}$$

Where C_0 is a constant that is used to normalize the mean intensity of the synthetic accelerograms to the intensity of original record.

A good measure of frequency content is the number of zero axis crossing per second. In order to determine the time variation of the frequency content of an earthquake record, the moving-time-window method is used. The time window size is assumed to be the same as the one used for the amplitude estimation. The zero-crossing rate at time t is defined as

$$\hat{F}_C(t) = \left(\text{Number of zero-crossing within the time interval } \left(t \pm \frac{t_w}{2}\right)\right)/t_w \tag{28}$$

Where t_w is the time-window size. A suitable algebraic time function is then fitted to the variation of the zero-crossing rate $\hat{F}_{Ca}(t)$ with time for each accelerogram. The time-dependent ground frequency function then is defined as

$$\omega_g(t) = \pi \hat{F}_{Ca}(t) \tag{29}$$

Obviously, lots of artificial records should be generated to achieve a reliable response of structure at dynamic analysis. The purpose of this method is to generate so many records compatible with the same spectrum. Generally, the main idea of this method is to use wavelet theory. The record decomposition results in coefficient sets of scaling Coefficients (cA), and wavelet coefficients (cD), which includes frequency contents.

Then, the nonstationary Kanai-Tajimi model is used to simulate the ground acceleration time history, and both the actual and simulated records are decomposed with discrete wavelet transforms (DWT). At the next step, the wavelet coefficients $cD_3 - cD_7$ of actual record replaced with the wavelet coefficients $cD_3 - cD_7$ of simulated record, because $cD_3 - cD_7$ contains most frequency contents, and finally the simulated record using inverse discrete wavelet transform is determined.

5. Analytical samples

The proposed model is used to produce artificial records for three Iranian earthquake accelerograms with different characteristics and four use records. These are Tabas 1978, Manjil 1990 and El Centro 1940 earthquakes.

For identifying the model parameters, window sizes 2, 2 and 1.5 seconds are used for the El Centro, Tabas and Manjil earthquakes, respectively. As noted before, the window size should be selected in such a way that it captures the time evolutions of the significant frequency content and the amplitude of the record. Also, 0.42, 0.35 and 0.3 are used respectively for the ground damping coefficient $\xi_g(t)$, for El Centro, Tabas and Manjil earthquakes (Fan and Ahmadi 1990, Tajimi 1960). A constant power spectral intensity of S_0 = 1cm^2/s^3 and time interval of Δt = 0.02 s, are used for white noise process generation. For each record, ensembles of 700 samples are generated and the value of C_0 is determined such that the expected total energy of synthetic accelerograms becomes equal to that of original record within the predetermined duration. Following this method, the values C_0 = 0.085, 0.0823 and 0.0564 ware found for the simulated El Centro, Tabas and Manjil earthquakes, respectively.

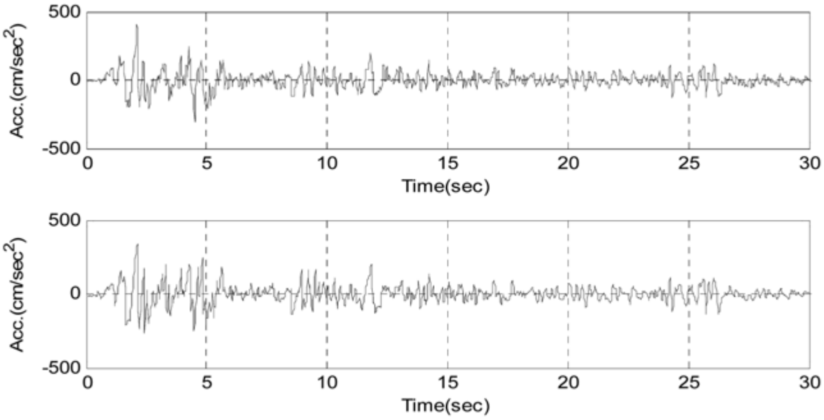

Fig. 1 Artificial (top) and actual (bottom) earthquake ground motion accelerograms of El Centro record

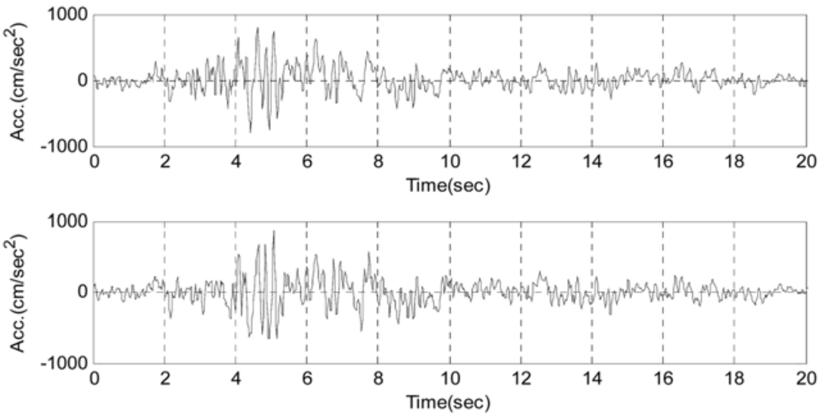

Fig. 2 Artificial (top) and actual (bottom) earthquake ground motion accelerograms of Tabas record

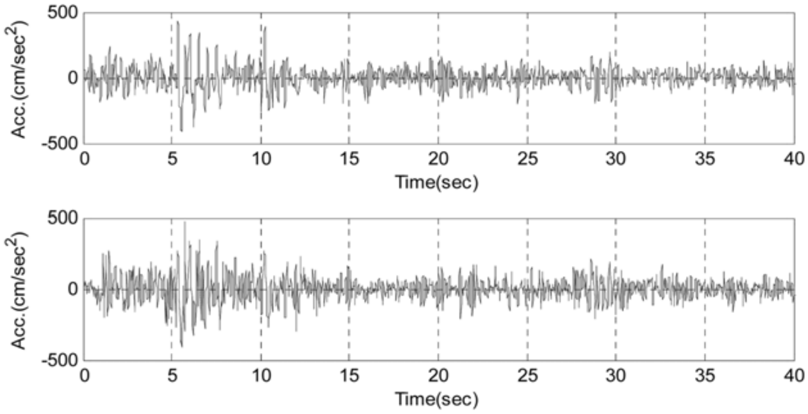

Fig. 3 Artificial (top) and actual (bottom) earthquake ground motion accelerograms of Manjil record

An ensemble of 50 synthetic accelerograms is generated and statically studied for each earthquake. It is noted that records have been decomposed with db-10 wavelet (the other wavelets could be applied). Figs. 1 to 3 compare the accelerograms of the actual El Centro, Tabas and Manjil earthquakes with the synthetically generated records.

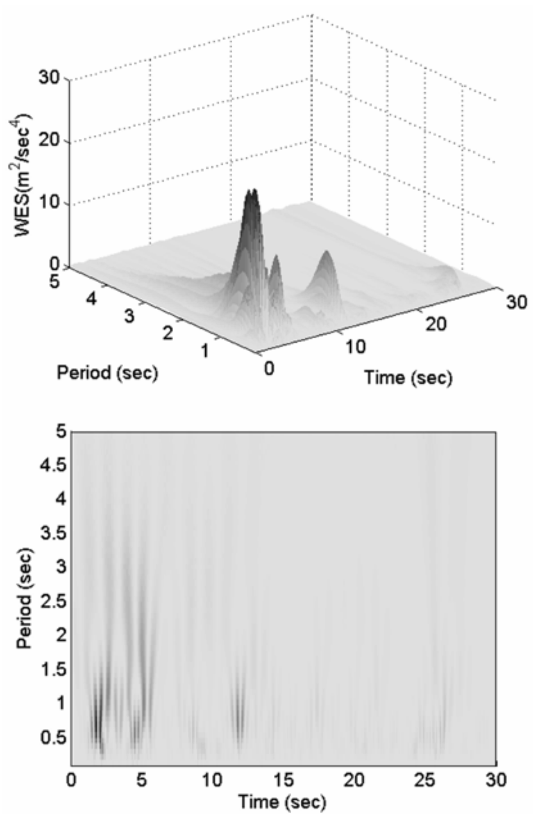

Fig. 4 Wavelet energy spectrum of actual earthquake accelerogram of El Centro record

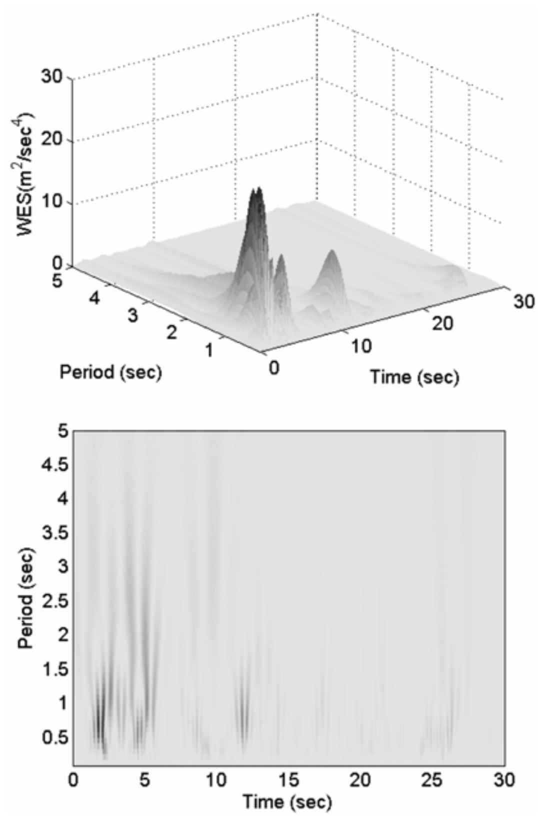

Fig. 5 Wavelet energy spectrum of artificial earthquake accelerogram of El Centro record

The WES of the actual and artificial accelerograms are displayed in Figs. 4 to 9 (MATLAB 1999). These figures show that the time evolutions of the frequency content of the actual and the generated accelerograms are comparable.

Next, statistical response spectra of the synthetic accelerograms are also compared with those of actual records. The equation governing the response of the SDOF structure under the ground acceleration a_g is given as (Naeim 1999)

$$\ddot{X} + 2\xi_0\omega_0\dot{X} + \omega_0^2 X = -a_g \tag{30}$$

where ω_0 and ξ_0 are the fundamental frequency and the damping coefficient of the SDOF. The pseudo-acceleration response spectrum is defined as

$$PSA(T_0, \xi_0) = \omega_0 \max\{X(t)\}, \quad T_0 = 2\pi/\omega_0, \quad \xi_0 = 0.05 \tag{31}$$

Figs. 10 to 12 compare the pseudo-acceleration response spectra and the related statistics for the ensemble of 50 simulated accelerograms with those for the actual records.

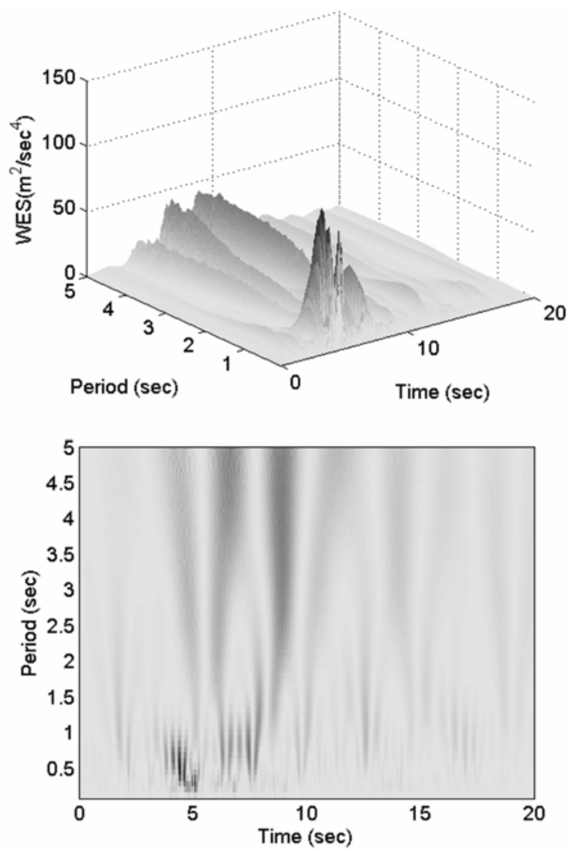

Fig. 6 Wavelet energy spectrum of actual earthquake accelerogram of Tabas record

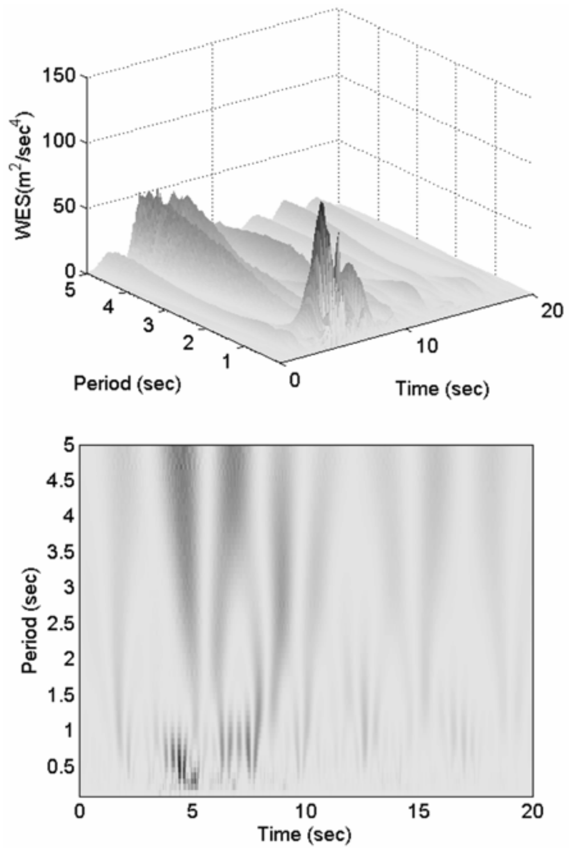

Fig. 7 Wavelet energy spectrum of artificial earthquake accelerogram of Tabas record

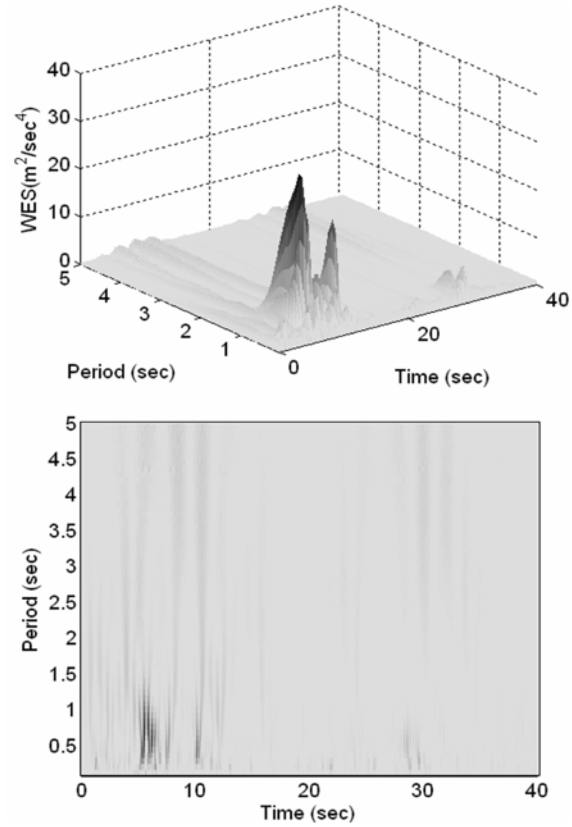

Fig. 8 Wavelet energy spectrum of actual earthquake accelerogram of Manjil record

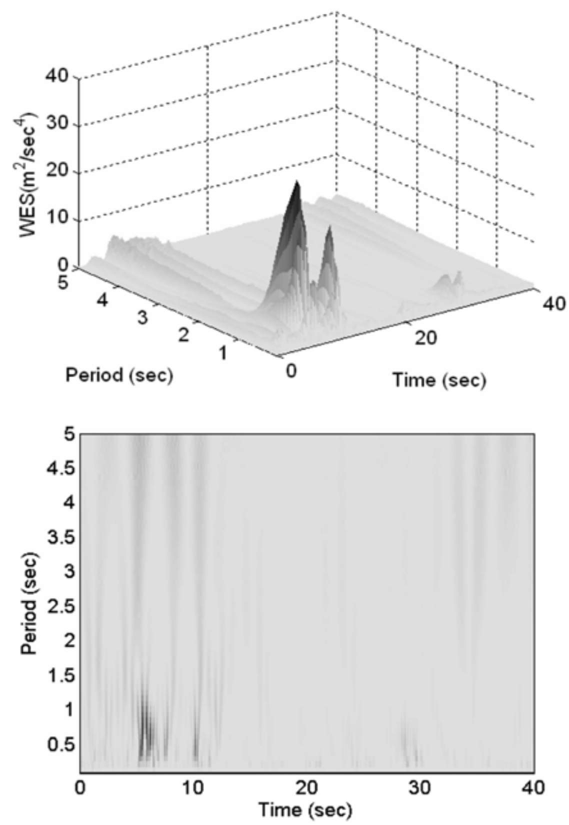

Fig. 9 Wavelet energy spectrum of artificial earthquake accelerogram of Manjil record

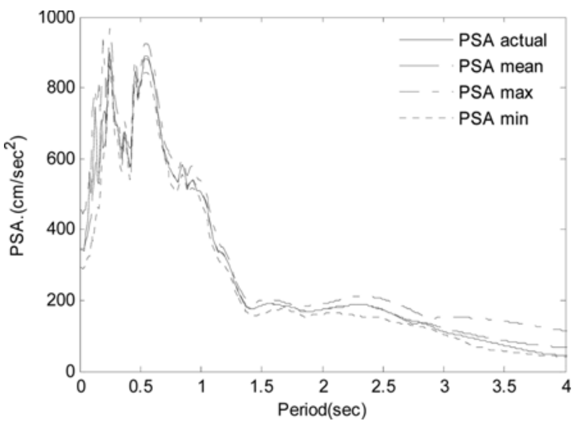

Fig. 10 Comparison between pseudo-acceleration response spectra of original and generated accelerograms for El Centro earthquake

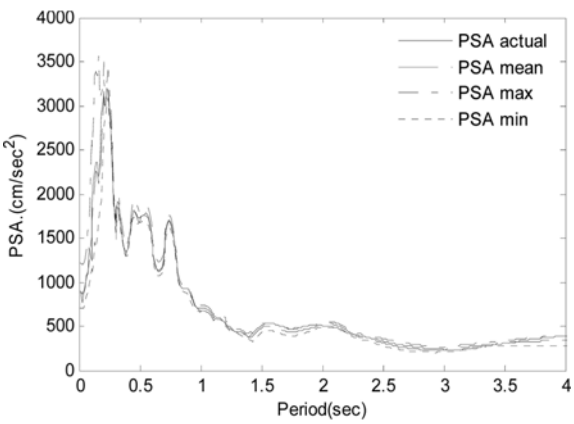

Fig. 11 Comparison between pseudo-acceleration response spectra of original and generated accelerograms for Tabas earthquake

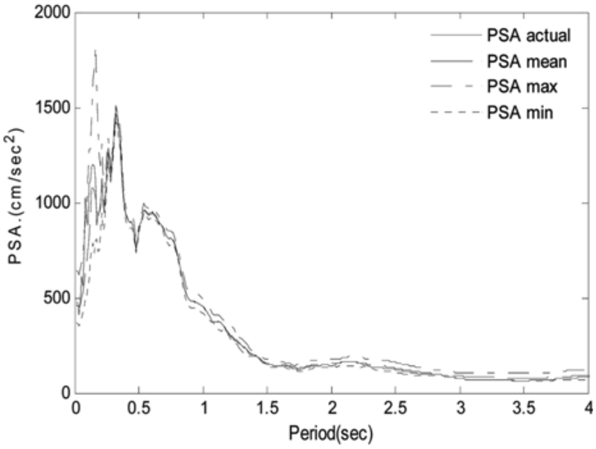

Fig. 12 Comparison between pseudo-acceleration response spectra of original and generated accelerograms for Manjil earthquake

Finally, the pseudo-acceleration response spectra and the related statistics for the ensemble of 50 simulated accelerograms with the model of this paper and the model of Fan and Ahmadi (1990) for El Centro 1940 earthquake record is compared in Fig. 13. Also, the pseudo-acceleration response spectra and the related statistics for the ensemble of 50 simulated accelerograms with the model of this paper and the model of Rofooei *et al.* (2001) for Tabas 1978 and Manjil 1990 earthquakes are compared in Figs. 14 and 15. It is shown that in all the pseudo-acceleration response spectra for the synthetic accelerograms with the model of this paper are close to those for the actual earthquakes.

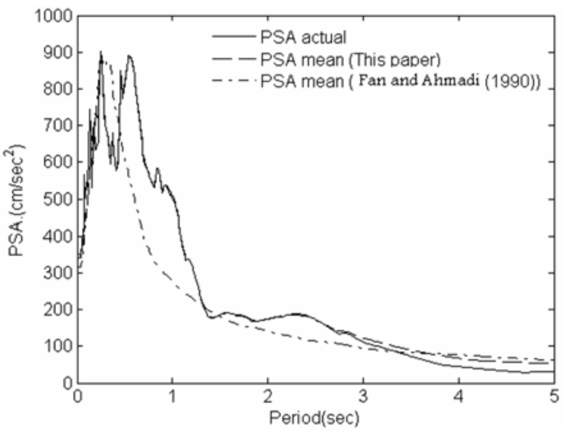

Fig. 13 Comparison between pseudo-acceleration response spectra of original and generated accelerograms, and other model for El Centro earthquake

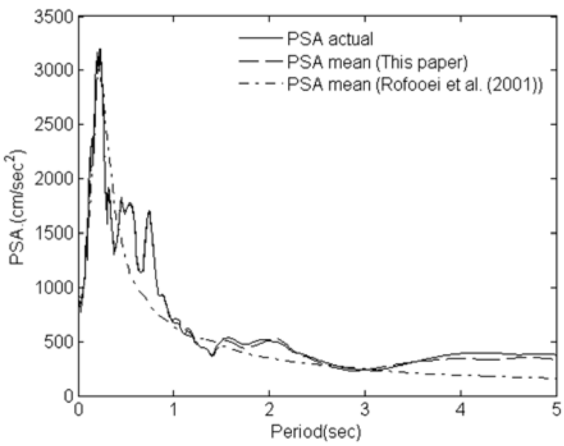

Fig. 14 Comparison between pseudo-acceleration response spectra of original and generated accelerograms, and other model for Tabas earthquake

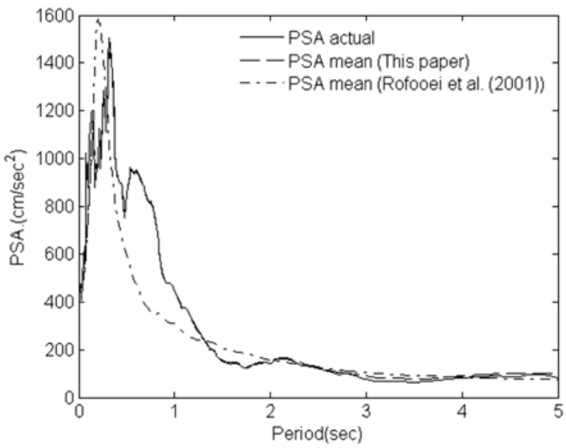

Fig. 15 Comparison between pseudo-acceleration response spectra of original and generated accelerograms, and other model for Manjil earthquake

6. Conclusion

In this study, a method of applying wavelet transform and generalized Kanai-Tajimi model for generation of artificial accelerograms for any site with at least one existing earthquake record is developed. This technique is based on using properties of wavelet transform and the generalized Kanai-Tajimi model to include the nonstationary evaluation of amplitude and dominant frequency of ground motion.

The model was used in generation of artificial earthquake records for El Centro, Tabas and Manjil earthquakes. A large number of synthetic accelerograms are generated and statistically analyzed. The suitability of the model is investigated based on the comparison of the characteristic of the generated accelerograms with those of the original ones. For comparison of the proposed model with other models, the result compared with previous models (Fan and Ahmadi 1990, Rofooei *et al.* 2001) and it is shown that the pseudo-acceleration response spectra for the synthetic accelerograms with the model of this paper are close to those for the actual earthquakes.

References

Ahmadi, G. (1979), "Generation of artificial time-histories compatible with given response spectra - A review", *SM Archives*, **4**, 207-239.

Daubechies, I. (1992), "Ten Lectures on Wavelets", *CBMS-NSF Conference Series in Applied Mathematics*, Montpelier, Vermont.

Fan, F.G. and Ahmadi, G. (1990), "Nonstationary Kanai-Tajimi models for El Centro 1940 and Mexico City 1985 earthquake", *Prob. Eng. Mech.*, **5**, 171-181.

Ghodrati Amiri, G., Ashtari, P. and Rahami, H. (2006), "New development of artificial record generation by wavelet theory", *Struct. Eng. Mech.,* **22**(2), 185-195.

Iyama, J. and Kuwamura, H. (1999), "Application of wavelets to analysis and simulation of earthquake motions", *Earthq. Eng. Struct. Dyn.*, **28**, 255-272.

Kanai, K. (1957), "Semi-empirical formula for the seismic characteristics of the ground motion", *Bull. Earth.*

Res. Inst. Univ. Tokyo, **35**, 309-325.
MATLAB Reference Guide (1999), The Math Works Inc.
Mukherjee, S. and Gupta, K. (2002), "Wavelet-based characterization of design ground motions", *Earthq. Eng. Struct. Dyn.*, **31**, 1173-1190.
Naeim, F. (1999), *The Seismic Design Handbook*, Van Nostrand.
Newland, D.E. (1994), Random Vibrations, Spectral and Wavelet Analysis, 3rd Edition, Longman Singapore Publishers.
Refooei, F.R., Mobarake, A. and Ahmadi, G. (2001), "Generation of artificial earthquake records with a nonstationary Kanai-Tajimi model", *Eng. Struct.*, **23**, 827-837.
Suarez, L.E. and Montejo, L.A. (2005), "Generation of artificial earthquake via the wavelet transform", *Solids Struct.*, **42**, 5905-5919.
Tajimi, H. (1960), "A statistical method of determining the maximum response of a building structure during an earthquake", *In: Proc. 2nd WCEE*, Vol. II. Tokyo: Science Council of Japan, 781-798.
Zhou, Z. and Adeli, H. (2003), "Wavelet energy spectrum for time-frequency localization of earthquake energy", *Comput. Aided Civil Infrastruct Eng.*, **13**, 133-140.

Notation

A_j	: Approximation at level j
a	: Scale parameter
$a_g(t)$	: Ground acceleration
b	: Translation parameter
C	: Constant
C_0	: Constant
CWT	: Continuous wavelet transform
cA	: Scaling Coefficients
cD	: Wavelet Coefficients
c_j	: jth coefficient of basis function
DWT	: Discrete wavelet transform
D_j	: Detail at level j
Δf	: Frequency interval
Δt	: Time interval
$\delta(\ )$	: Dirac delta function
E	: Earthquake energy input
$E[]$	: Expected value
$e(t)$	: Amplitude envelope function
FFT	: Fast Fourier transform
$\hat{F}_C$	: Zero-crossing rate
$\hat{F}_{Ca}(t)$	: A suitable algebraic time function is then fitted to the variation of the Zero-crossing rate
f	: Center frequency
$n(t)$	: A stationary Gaussian white noise process
ξ_0	: Damping coefficient of the SDOF
ξ_g	: Site dominant damping coefficient
$\xi_g(t)$	: Effective ground damping coefficient
PSA	: Pseudo-acceleration response spectrum
S	: Spectral density function
S_0	: Constant power spectral intensity of bedrock excitation
STFT	: Short Time Fourier Transforms
σ	: Standard deviation
$\sigma_a(t)$	: A smooth algebraic time function is fitted to the time variation of the Standard deviation
t	: Time

t_w	: Time-window size
W	: Continuous wavelet transform coefficients
WES	: Wavelet energy spectrum
$\phi(t)$	: Scaling function
X	: Displacement
$\dot{X}$	: Velocity
$\ddot{X}$	: Acceleration
X_f	: Filtered response
$\ddot{X}_g$	: Output ground acceleration
Ψ	: Fourier transform of ψ
ψ	: Basis function
ψ^*	: Complex conjugate of ψ
ω	: Frequency
ω_0	: Fundamental frequency of the SDOF
ω_g	: Site dominant frequency
$\omega_g(t)$	: Time dependent ground frequency